THE EFFECT OF LEG SEGMENTAL PROPORTIONS ON THE ENERGETIC COST OF ROBOTIC LOCOMOTION

PANAGIOTIS CHATZAKOS AND EVANGELOS PAPADOPOULOS

Department of Mechanical Engineering, National Technical University of Athens
Athens 157 80, Greece

In this paper the influence of knee joint on the motion of the robot and the effect of leg segmental proportions and angle between leg segments on the performance of the robot is explored via parametric analysis. The spring loaded inverted pendulum (SLIP) running in the sagittal plane, which is a simple model commonly used to analyze the basic qualitative properties of running, is used. The performance index is the cost of locomotion, which is given as the actuator power to sustain a certain motion, very close to a passive one, normalized to forward velocity per body length and robot weight. Simulation results show that the effect of leg configuration is great and that considerable variations exist on the value of the energetic cost of locomotion that makes some leg configurations more desirable than others.

1. Introduction

A number of legged robots such as, the MIT quadruped ([1]), the RHex ([2]), the Scout II ([3]), and the Tekken ([4]), have been built with different physical parameters and leg configurations. Despite the large number of publications, the interesting issue of what type of leg, straight or segmented, is best for robotic locomotion remains still relatively untouched. Also, the influence of knee joint on the motion of the robot and the effect of leg segmental proportions and angle between leg segments on the performance of the robot is not fully explored.

Lee and Meek in [5] examined the effects of joint orientation on individual leg forces and centre of mass dynamics. Rummel et. al. in [6] suggested that depending on segmental orientation with respect to the movement direction legs can (a) increase their mechanical advantage or (b) increase the elastic capacity of the leg. In [7] the question of the influence of leg segmentation (i.e. the use of rotational joint and two limb-segments) to the self-stability of running was addressed and self-stable running behavior in significantly broader ranges of running speed and control parameters was showed.

In this paper, the goal is to gain better insight into legged locomotion focusing on segmented legs and their influence on robot performance. Simulation results show that the effect of leg configuration, i.e., leg segmental

proportions and angle between leg segments, is great and that considerable variations exist on the value of the energetic cost of locomotion that make some leg designs more desirable than others. Also, the internal forces developed, especially in the vicinity of singular positions of the leg mechanism are considered. It appears that the common design principle in nature, i.e., the use of knee joint and two limb-segments is the basis for economical, in the wider sense, running.

The study in this paper is based on a parametric analysis of leg configuration and examines the behavior of the energetic cost of locomotion over a range of robot parameters. The spring loaded inverted pendulum (SLIP) running in the sagittal plane, which is a simple model commonly used to analyze the basic qualitative properties of running, is used ([8]). The cost of locomotion is based on the actuator power to sustain a certain motion, very close to a passive one, normalized to forward velocity per body length and robot weight ([9]). Also, singularities that represent leg configurations at which mobility of the leg structure is reduced and internal forces are large were penalized. This paper shows that the effort of the robot to execute a particular motion changes across the parametric region of leg physical parameters. Findings from simulation results indicate that make some parametric regions, i.e., leg segments proportion and the space between leg segments, are more desirable than others, and thus their study can facilitate improved legged robot design.

2. System Dynamics

As shown in Figure 1, the planar model consists of a rigid body and one springy massless leg, attached to the body. An actuator controls the angle of the leg with respect to the body and the torque delivered by the leg. The modeled leg represents the virtual leg, [1], in which all the legs are always in phase.

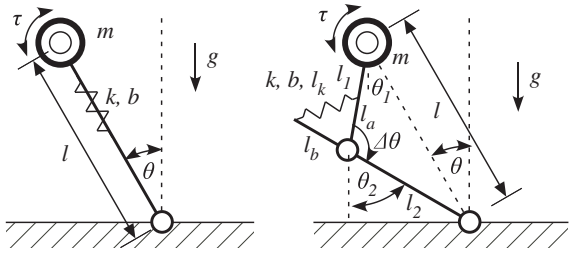

Figure 1. Parameters of the template for running in plane, straight (left) and segmented (right) leg.

System dynamics are derived using a Lagrangian approach. During flight, the robot is under the influence of gravity only. Throughout the stance phase, the

robot's toe is fixed on the ground, and acts as lossless pivot joint. The dynamics for flight may be derived from that of the stance, by removing appropriate terms. Here, only the stance dynamics is given, in the form of a set of differential and algebraic equations, for the straight leg and the segmented leg, respectively,

$$\begin{aligned} ml^2\ddot{\theta} + 2m\dot{l}l\dot{\theta} - mlg\sin\theta = \tau \\ m\ddot{l} - ml\dot{\theta}^2 + b\dot{l} + k(l - l_o) + m\lg\cos\theta = 0 \end{aligned} \tag{1}$$

$$\begin{aligned} ml^2\ddot{\theta} + 2m\dot{l}l\dot{\theta} - mlg\sin\theta = \tau \\ m\ddot{l} - ml\dot{\theta}^2 + b_k\dot{l}_k^2 + k_k(l_k - l_{ko})\dot{l}_k + m\lg\cos\theta = 0 \end{aligned} \tag{2}$$

Next, the conservative models of Eqs. (1) and (2) are considered. These are called the passive dynamics of the system and encode the target behavior of the system and reveal intrinsic system properties and aspects of running that may be used as guidelines for the design of legged robots. The passive and conservative model of our analysis is derived from Eq. (2) by eliminating actuation and energy dissipation terms.

On this model, we employ dimensional analysis in order to reveal the effect of scaling of similarly configured systems and widen our study. Dimensional analysis can be applied to all quantitative models and offers an efficient way to display complex data sets. Usually, it makes the subsequent analysis much more useful, because the physical model, as first written, is rather general. The premise of dimensional analysis is that complete equations can be written in a form that is independent of the choice of units, and variables appear in combinations that are dimensionless. Such dimensionless variables are introduced as follows,

$$t^* = \frac{t}{s} \tag{3}$$

$$x^* = \frac{x}{l_o},\ \dot{x}^* = s\frac{\dot{x}}{l_o},\ \ddot{x}^* = s^2\frac{\ddot{x}}{l_o} \tag{4}$$

$$y^* = \frac{y}{l_o},\ \dot{y}^* = s\frac{\dot{y}}{l_o},\ \ddot{y}^* = s^2\frac{\ddot{y}}{l_o} \tag{5}$$

$$\theta^* = \theta,\ \dot{\theta}^* = s\dot{\theta},\ \ddot{\theta}^* = s^2\ddot{\theta} \tag{6}$$

where s is the time scale of the system, and the rest of the variables are defined in Table 1.

By substituting (3)-(6) into the equations of motion, given by (2) for the segmented leg, one gets a dimensionless description of the system. The resulting motion of the COM is characterized by a time scale, which is associated to the inverse of the natural frequency of the horizontal oscillation motion,

$$s = \sqrt{\frac{l_o}{g}} \tag{7}$$

Selection of (7) as the time scale of the system, results to a dimensionless parameter, which is widely used by experimental biologists, namely relative stiffness defined as

$$r = \frac{k\, l_o}{m\, g} \tag{8}$$

The rest of system parameters, that is the torque delivered at hip and the dimensionless viscous friction coefficient b^*, are normalized as

$$\tau^* = \frac{\tau}{mg\, l_o} \tag{9}$$

$$b^* = \frac{b}{m}\sqrt{\frac{l_o}{g}} \text{ or } b^* = 2\zeta\sqrt{r} \tag{10}$$

where ζ is the damping ratio.

Table 1. Variable and indices used.

Symbol	*Units*	*Variable*	*Symbol*	*Units*	*Variable*
x	m	horizontal pos.	T	s	cycle duration
y	m	vertical pos.	Ts	s	stance duration
θ	^{o}	leg angle	g	m/s^2	gravity
l	m	leg length	m	Kg	body mass
lo	m	leg free length	r	-	relative stiffness
k	N/m	spring stiffness	s	s	time scale
b	N.m/s	spring damping	k	-	index: knee
τ	N.m	torque delivered	*	-	index: dimensionless

3. Periodic Trajectories

In order to evaluate the performance of the above model, we focus on system periodic steady state trajectories, which are identical trajectories that repeat themselves during locomotion. Following a similar procedure as in [9] we employ a Poincaré Map technique to formulate these trajectories. The return map connects the system state at a well-defined locomotion event to the state of the same event at the next cycle. Here, this event is chosen to be the apex height, because the vertical velocity is always zero there. Furthermore, the distance traveled has no influence on the locomotion cycle. Thus, the state vector $\mathbf{x}^*$ at apex height consists of the apex height y^* and the forward speed $\dot{x}^*$ only, i.e.,

$$\mathbf{x}^* = \begin{bmatrix} y^* & \dot{x}^* \end{bmatrix} \tag{11}$$

The state vector at apex height for some cycle n, $\mathbf{x}_n^*$, constitutes the initial conditions. Based on these, the flight equations, derived from (2) for the segmented leg by removing terms not permanent to the phase, are integrated until one of the touchdown events occurs. The touchdown event triggers the next phase, whose dynamics are integrated using as initial conditions the final conditions of the previous state.

Successive forward integration of the dynamic equations of all the phases yields the state vector at apex height of the next stride, which is the value of the Poincaré return map **F**. If the state vector at the new apex height is identical to the initial one, the cycle is repetitive and it is yields a fixed point. Mathematically, this is given as

$$\mathbf{x}_{n+1}^* = \mathbf{F}\left(\mathbf{x}_n^*\right) \tag{12}$$

It must be noted that existence of such fixed points seems to be the rule, rather than the exception.

In order to determine the conditions required to result in steady state cyclic motions, we resort to a numerical evaluation of the return map using a Newton-Raphson method. By employing this method, a large number of fixed points can be found for different initial conditions and different touchdown angles. These angles, although they are not part of the state vector $\mathbf{x}_n^*$, and are not generalized coordinates, they directly affect the value of the return map as they determine touchdown and liftoff events and impose constraints on the motion of robot during stance phase. Variant combinations of robot parameters, as defined in Figure 1, result also to different fixed points.

4. Performance Index

Following these assumptions, the robot executes a passive motion according to the sets of initial conditions found and no energy is lost or added to the system. Surprisingly, if one uses actuators just to compensate for the energy lost and initial conditions that yield a passive trajectory the robot will execute an active gait very close to the passive gait and the system can be studied as in the lossless case. Then, the only energy required to sustain the motion is the amount dissipated over one stride, *E*, which is the sum of the energy dissipated due to friction at legs E_m and the kinetic energy lost in ground at touchdown E_g.

The dimensionless mechanical energy losses due to leg friction are found using (13) to be

$$E_m^* = b^* \int_0^{T_s} i^{*2} dt^* \tag{13}$$

In addition to friction losses, energy losses due to the interaction of robot's legs with the ground exist. Particularly, the running robot dissipates some of its kinetic energy in ground damping and compression at touchdown. Ground surface is modeled as a parallel spring-damper system that influences the robot only when the feet are in contact with the ground, i.e., when the vertical velocity is negative. The acting direction of ground spring-damper system is along the direction of robot's interacting leg. Each time the foot touches the ground, the rest position of the ground spring is reset to the point at which the foot first touches. The coefficient of friction between the foot and the ground is assumed to large, so that slipping never occurs. Finally, for a wide yet reasonable range of damping and stiffness coefficients, the ground displacement (deformation) is negligible compared to leg length, and the integrated robot and ground motion equations can be approximated by (2) for the segmented leg and (36),

$$b_g^* \dot{l}_g^* + r_g l_g^* = r\left(l^* - 1\right) \tag{14}$$

To this end, the dimensionless ground energy losses due to ground damping and ground permanent deformation are found using (15) to be,

$$E_g^* = \int_0^{T_s} b_g^* \dot{l}_g^{*2} dt^* \tag{15}$$

In our analysis, distance covered is of the major consideration, and thus the energy cost for moving a unit distance is considered. Since the rate of dissipated energy per unit time is the required power P to sustain the motion over one cycle, and since the rate of distance covered per unit time is the forward speed of locomotion v, normalizing the power cost for moving with unit speed to the robot weight mg, yields a dimensionless criterion, the specific resistance, [10], as,

$$e = \frac{P}{mgv} \tag{16}$$

The specific resistance is a good overall criterion that can be used for optimizing mobile robot designs. To analyze this effect in the dimensionless framework, i.e., using dimensionless parameters, so as to reveal the effect of scaling in determining robot physical parameters, we define a variation of e, the dimensionless cost of locomotion e^*,

$$e^* = \frac{P^*}{v^*} = \frac{E^*}{T^* v^*} \tag{17}$$

where P^* is the dimensionless required mean power to sustain the passive motion over one cycle or alternatively the dimensionless energy dissipated over one stride E^* divided by cycle duration T^*, and v^* the dimensionless forward speed of

the robot. Therefore, leg segmental proportions and the angle between leg segments should be chosen so that Eq. (17) is minimized.

If the segmented leg is seen as a two-link manipulator, then leg configurations at which mobility of the structure is reduced and the internal forces developed are increased (namely internal singularities) should be avoided. On the basis of penalizing such configurations and maximizing mobility, a generally accepted measure of mobility (and force transmissibility) ω is adopted,

$$\omega = \sqrt{\det\left(\mathbf{J}\left(\mathbf{q}\right)\mathbf{J}^{T}\left(\mathbf{q}\right)\right)} \tag{18}$$

which should be maximized in order to move away from internal singularities. Although in a dimensional frame the numerical value of (18) does not constitute an absolute measure of actual closeness of the structure to a singularity, here this does not apply as dimensionless variables and parameters are used; thus greater values of (18) correspond to "better behaved" structures.

To this end, the performance index is defined as the weighted sum of relative mobility measure, i.e., divided by the maximum permissible, and relative cost of locomotion, namely

$$\text{P.I.} = w_{\omega}\frac{\omega}{\max\left(\omega\right)} + w_{e}\frac{e^{*}}{\min\left(e^{*}\right)} \tag{19}$$

By using (19) one can identify that combination of robot dimensionless parameters, for which the P.I. is least, and thus obtain the optimal leg segmental proportions and angle between leg segments.

5. Results

In this section, the results of the parametric analysis are presented. The results are obtained by simulation for a parametric range of (a) robot leg segmental proportions and the space between leg segments; see Figure 2 left, and (b) placement of the linear spring along the two leg segments.

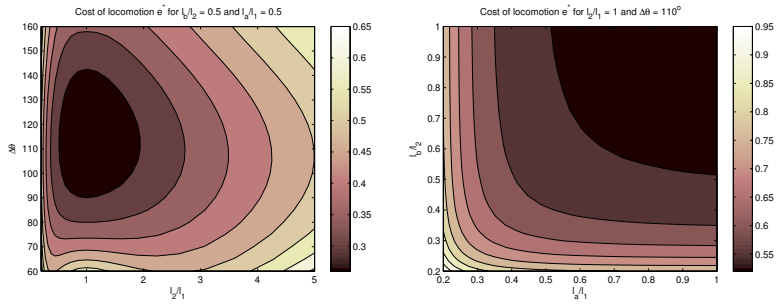

Figure 2. The effect of leg segments proportion and the space between leg segments on performance.

Considerable variations do exist on the value of the energetic cost of locomotion that makes some leg configurations more desirable than others. The configuration of an equally segmented leg that forms an internal angle of approx. 110^o is found to be optimal. This is a very interesting result, which suggests that the results of the analysis presented in this work can also explain the biological designs found in nature, i.e., the use of knee joint and two limb-segments.

Acknowledgments

Partial support of this work by public (European Social Fund 75% and General Secretariat for Research and Technology 25%) and private funds (Zenon SA), within measure 8.3 of Op. Pr. Comp., 3rd CSP-PENED 2003 is acknowledged.

References

1. Raibert, M. H., "Legged Robots that Balance", MIT Press, 1986.
2. Saranli, U., Buehler M., and Koditschek D.E., "RHex: A Simple and Highly Mobile Hexapod Robot", in the Int. J. of Robotics Research, Vol. 20, No. 7, 2001, pp. 616-631.
3. Poulakakis, I., E. Papadopoulos and M. Buehler, "On the Stability of the Passive Dynamics of Quadrupedal Running with a Bounding Gait,", in the Int. J. of Robotics Research, vol. 25, no. 7, 2006, pp. 669-687.
4. Kimura, H. , Y. Fukuoka and A. H. Cohen, "Adaptive Dynamic Walking of a Quadruped Robot on Natural Ground Based on Biological Concepts,", in the Int. J. of Robotics Research, vol. 26, no. 5, 2007, pp. 475-490.
5. Lee D. V. and Meek S. G., "Directionally compliant legs influence the intrinsic pitch behaviour of a trotting quadruped", in the Proc. R. Soc. B 272, 2005, pp. 567–572.
6. Rummel J., Iida F. and Seyfarth A., "One-Legged Locomotion with a Compliant Passive Joint", Intelligent Autonomous Systems, Arai et al. (Eds.), IOS Press, 2006.
7. Rummel J., Iida F., Smith J. A. and Seyfarth A., "Enlarging Regions of Stable Running with Segmented Legs", 2008 IEEE International Conference on Robotics and Automation Pasadena, CA, USA, May 19-23, 2008.
8. Full R. J. and Koditschek D., "Templates and Anchors: Neurome-chanical Hypotheses of Legged Locomotion in Land", in the J. of Experimental Biology, Vol. 202, 1999, pp. 3325-3332.
9. Chatzakos P. and Papadopoulos E. G., "Parametric Analysis and Design Guidelines for a Quadruped Bounding Robot", in Proc. of the 15th Mediterranean Conf. on Control and Automation, 2007, Greece.
10. Gabrielli, G. and von Karman T., "What price speed?", in the Mechanical Engineering, ASME, Vol. 72 (10), 1950.